Plasmonics
DOI 10.1007/s11468-012-9349-1

Controlled Fabrication of Gold Nanoparticle and Fluorescent Protein Conjugates

Gili Bisker · Limor Minai · Dvir Yelin

Received: 21 December 2011 / Accepted: 5 March 2012

Abstract The unique optical properties of gold nanoparticles make them attractive for a wide range of applications which require optical detection and manipulation techniques. Here, we experimentally demonstrate the use of single femtosecond pulses at resonance wavelength for a controlled conjugation of gold nanoparticles and fluorescent proteins. This optically driven reaction is rigorously studied and analyzed using a variety of experimental techniques, and a detailed model is proposed which describes the adsorption of the proteins onto the nanoparticles' surface, as well as their subsequent desorption by a reducing agent. Potential applications of the resulting nanoparticle–protein conjugates include controlled delivery of fluorescent markers and local sensing of biochemical processes.

Keywords Gold nanoparticles · Femtosecond pulses · Plasmon resonance · Fluorescent proteins

Introduction

Gold nanoparticles play an important role in recent biomedical research and applications due to their small dimensions and high biocompatibility [1]. A single coating agent or a combination of several chemical compounds are often used to improve the particles' chemical and physical stability, increase their targeting specificity, and enhance their overall functionality [2–4]. Examples of such coatings include layers of polyethylene glycol (PEG) [5, 6], cetyltrimethylammonium bromide [7], peptides, and specific antibodies with high affinity to various targets such as epidermal cells [8–10], breast adenocarcinoma tumor cells [11], and lymphoma cells [12]. Functionalized gold nanoparticles have also been demonstrated useful for delivering conjugated pharmaceutical agents to specific targets [13, 14].

Additional important features of gold nanoparticles include unique absorption and scattering resonances in the visible–near infrared wavelength range [15, 16]. Interactions between laser irradiation and gold nanoparticles have been utilized for multiphoton imaging [17], ablation of human chromosomes [18], protein degradation [19, 20], and photothermal therapy of cancer [21, 22]. When resonantly illuminated with intense short laser pulses, gold nanoparticles can directly affect their nearby environment through a variety of physical mechanisms, including near-field enhancement [23–26], local heating [27], generation of acoustic shock waves [28], and the formation of cavitation bubbles [29]. High-power pulse lasers were recently demonstrated useful for assisting the synthesis process of gold nanoparticles [30–34] and for tuning their size and morphology [35–38].

Using gold nanoparticles and fluorescent molecules in a single chemical complex could provide further control over the fabrication, delivery, and functionality of such substances [39]. Quenching of fluorescent molecules when in close proximity to a nanoparticle, a process which was extensively studied both theoretically [40, 41] and experimentally [42, 43], could provide valuable insights on the exact particle–chromophores interaction on a nanometric scale. Monitoring the fluorescence signal of gold nanoparticles and green fluorescent protein (GFP) complexes, which were fabricated in a two-step reaction using positively charged ligands [44, 45], has been utilized for detecting different

Electronic supplementary material The online version of this article (doi:10.1007/s11468-012-9349-1) contains supplementary material, which is available to authorized users.

G. Bisker (✉) · L. Minai · D. Yelin
Department of Biomedical Engineering,
Technion–Israel Institute of Technology,
32000 Haifa, Israel
e-mail: bisker@tx.technion.ac.il

Published online: 20 March 2012

proteins in human serum [44] and for differentiating between cancerous cells [45]. Highly uniform GFP-coated gold nanoparticles were recently synthesized in a single-step chemical procedure using chloroauric acid and silver nitrate, where the fluorescent signal was utilized for monitoring the synthesis process [46].

Recently, a new approach for the production of functionalized gold and silver nanoparticles was demonstrated [37, 47, 48], using high-power femtosecond laser illuminating a bulk surface in the presence of a liquid medium which contains the functionalizing molecules. The high level of both chemical and optical control parameters offered by this technique allow high throughput and provide valuable flexibility in the design of the final conjugates [49, 50]. In some cases, however, it may be desired to selectively adsorb specific molecules onto existing nanoparticles; such a process could be also triggered and controlled by laser irradiation. The benefits of such step-by-step hybrid approach include high particle uniformity, high level of control, and low production cost.

In this work, we experimentally study and demonstrate a laser-driven chemical process for a controlled conjugation of gold nanoparticles to different fluorescent protein molecules. The process was enabled by illuminating PEG-coated nanoparticles with intense single ultrashort laser pulses at wavelengths that were tuned to their plasmonic resonance, while monitoring the signal emitted from the fluorescent proteins. Following the single-pulse irradiation, the fluorescent proteins were rapidly adsorbed onto the gold nanoparticles' surface, replacing the original PEG coating layer. The immediate fluorescence quenching and spectral changes provided real-time verification for the adsorption process.

Experimental System

PEG is a hydrophilic coating favorable for biomedical applications since it can be readily used as a biocompatible cross linker to different functional groups and antibodies [6, 12, 51, 52]. PEG-coated gold nanoparticles of 20 nm in diameter were prepared by trisodium citrate reduction of hydrogen tetrachloroaurate trihydrate salt followed by ligand exchange, where polyethylene glycol conjugated to thioctic acid (PEG-TA) replaced the citrate capping [5, 6]. The resulting coated nanoparticle solution (1.4×10^{-9} M) was then mixed with 3.4×10^{-6} M fluorescent protein solution and placed in a 0.75-mm-thick glass chamber on a motorized stage of an inverted microscope. A similar procedure was repeated for seven different fluorescent proteins which share a similar conformation, including GFP, blue fluorescent protein (BFP), cyan fluorescent protein (CFP), enhanced green fluorescent protein (EGFP), yellow fluorescent protein (YFP), dsRED, and mCherry. Mole ratios of approximately 1:2,400 were kept between the nanoparticles and the protein molecules.

The sample was illuminated (Fig. 1) by directing (mirror M1) a slowly focused beam of 50-fs pulses from an optical parametric amplifier (Topas, Newport Corp.), producing a 1-mm-diameter spot on the solution chamber. The pulse central wavelength was tuned to 545 nm for matching the plasmonic resonance frequency of the 20-nm-diameter gold nanospheres. The fluence of a single pulse was approximately 33 mJ/cm^2 (6.6×10^{11} W/cm^2), adjusted by changing the distance between the focusing lens (500 mm focal length) and the sample and by using a variable neutral density (ND) filter. Lateral raster scanning at 3 Hz line rate of the 330-μm-diameter beam (100-Hz pulse repetition rate) resulted in the illumination of the entire sample volume ($11\times11\times0.75$ mm) with a single pulse at each spot.

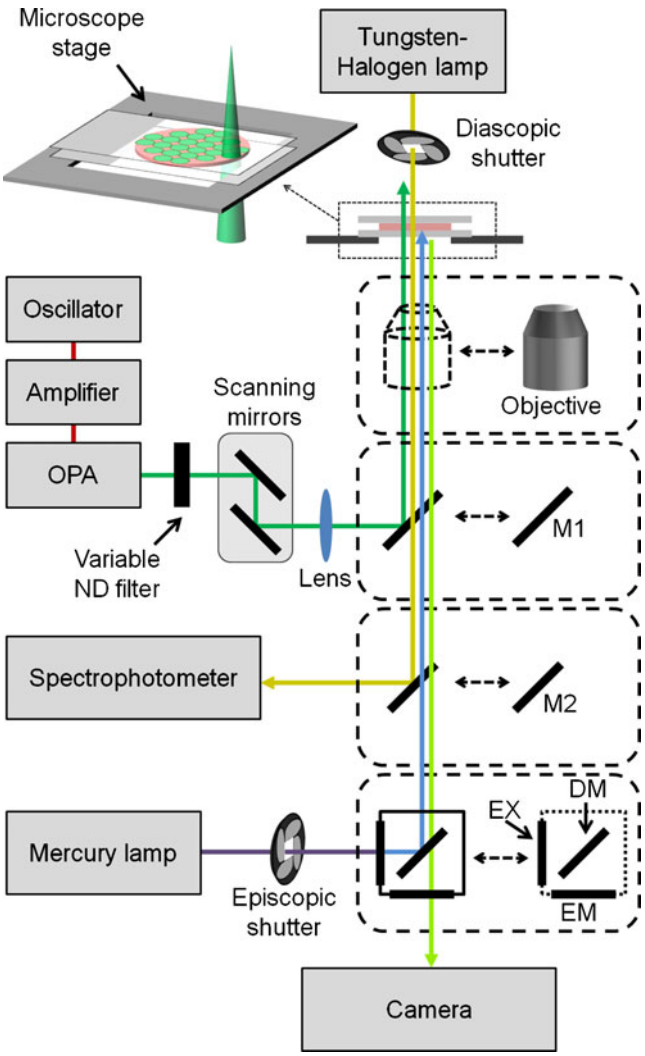

Fig. 1 Schematic illustration of the experimental system for laser-driven adsorption of fluorescent proteins on gold nanoparticles. *M1*, *M2* broadband mirrors, *ND* neutral density, *EX* excitation filter, *EM* emission filter, *DM* dichroic mirror, *OPA* optical parametric amplifier

After illumination, an objective lens (NA=0.13) was placed back at the main optical path for imaging the fluorescence distribution on a CCD camera, while different combinations of filters and dichroic mirrors were used to match the spectra of the different fluorescent proteins.

Results

The fluorescence emission of each protein–nanoparticle solution following illumination by single femtosecond pulses showed a pattern of dark regions which corresponded to the array of the illumination spots (Fig. 2a). The relative changes in fluorescence were calculated according to $(I - I_i)/I_i$, where I_i and I denote the averaged fluorescence pixel value before and after pulse illumination, respectively, and plotted on a bar chart in Fig. 2b. A consistent drop of the fluorescence signal following irradiation was measured for all solutions, ranging from 17 % for the nanoparticle–BFP solution up to 51 % for the nanoparticle–GFP solution, whereas most protein solutions in the absence of nanoparticles showed much smaller fluorescence reductions.

In order to shed light on the underlying process and show that the loss of fluorescence resulted from protein adsorption on the nanoparticles, the illuminated solutions have been further analyzed using light spectroscopy, electron microscopy, gel electrophoresis, western blotting, and mass spectrometry. Extinction spectra of the irradiated solutions were measured in transmission mode using a tungsten–halogen lamp at the microscope's diascopic illumination system and a commercial spectrophotometer (USB4000, Ocean Optics Inc.) which was attached to one of the microscope ports (see Fig. 1). The spectra of the GFP–nanoparticle solution (Fig. 3) after a single-pulse illumination (solid blue line) revealed a noticeable 22-nm narrowing and 7-nm blue shift of the plasmonic peak, compared to the spectrum before illumination (dashed blue line). Such spectral changes could be attributed to structural changes of the nanoparticles [36] and partial removal of the particles' coating layer [53–56]. In contrast, the extinction spectrum of a pure PEG-coated nanoparticle solution (no fluorescent proteins) showed significant loss of the plasmonic peak (solid green line) following irradiation, indicating the formation of large aggregates [57]. A similar loss of the plasmonic peak was observed following pulse illumination of PEG-coated nanoparticles in the presence of myoglobin (solid black line) and streptavidin (solid red line), two non-fluorescent proteins of molar concentrations similar to that of the fluorescent protein solutions.

Transmission electron microscopy (TEM, Tecnai Inc.) of the remaining portion of the nanoparticle–GFP solution after single-pulse irradiation has confirmed that the particles did not form aggregates (Fig. 3, left inset), while large aggregates were observed throughout the sample in the absence of GFP (Fig. 3, right inset), in agreement with the observed loss of the plasmonic peak (Fig. 3, solid green curve).

For quantifying the effect of the laser pulses on the fluorescent protein molecules, sodium dodecyl sulfate polyacrylamide gel electrophoresis (12 % Tris–glycine) of the irradiated nanoparticle–GFP solutions was performed, followed by Coomassie brilliant blue staining (Fig. 4a). With no reducing agent added to the solution prior to gel electrophoresis, a monotonic decrease of the main GFP band at 28 kDa was observed for increasing pulse fluence (Fig. 4b, blue diamonds), which correlated well with the observed

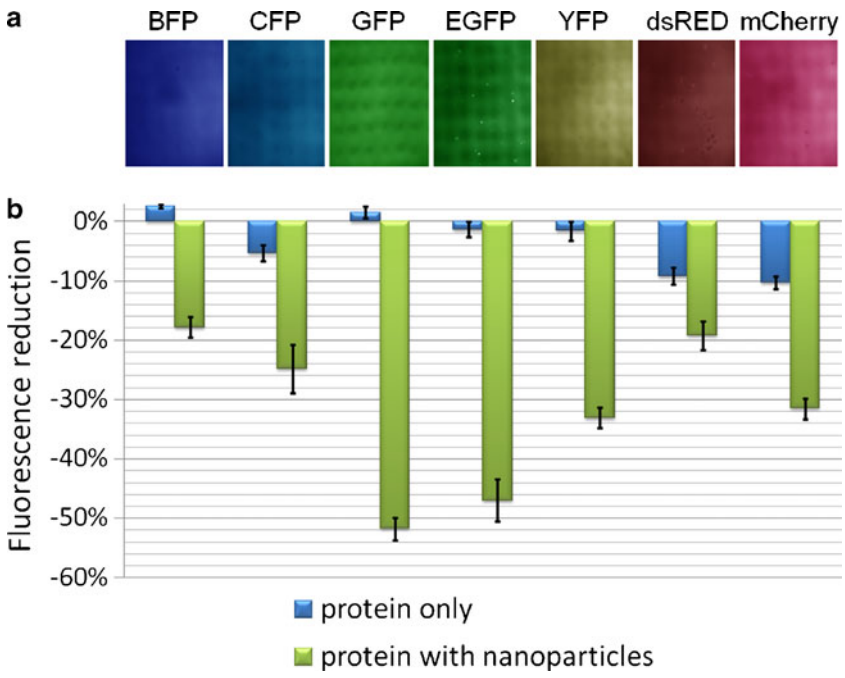

Fig. 2 **a** Fluorescence images of the nanoparticle–protein solutions following resonant illumination by a single pulse. The (false) colors correspond to the fluorescence emission wavelength of each protein. The field of view of each frame is 2.5×1.87 mm. **b** A bar chart showing the relative changes of the total fluorescence intensities after laser irradiation for protein-only solutions (*blue bars*) and for nanoparticle–protein solutions (*green bars*)

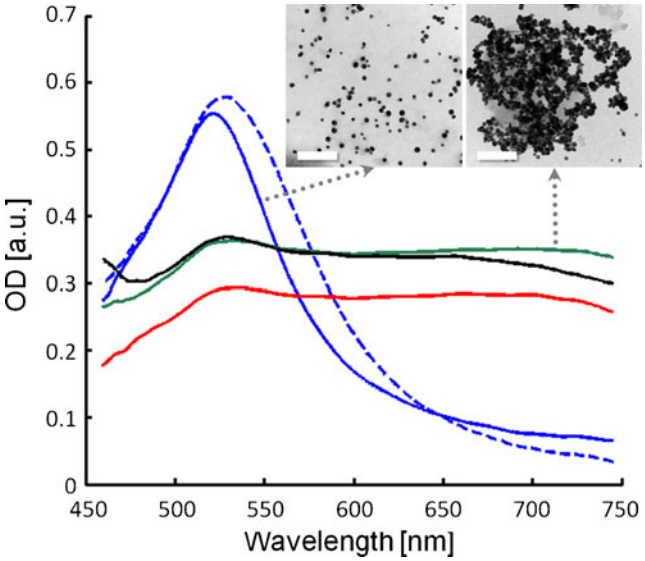

Fig. 3 Extinction spectra of illuminated nanoparticle solution with GFP before (*dashed blue curve*) and after a single-pulse illumination (*solid blue curve*). Loss of the absorption peak after a single-pulse irradiation was observed when the nanoparticles were mixed with myoglobin (*solid black curve*), streptavidin (*solid red curve*), and without proteins (*solid green curve*). *Left inset*: TEM image of an irradiated nanoparticle–GFP solution. *Right inset*: TEM image of irradiated gold nanoparticles in the absence of fluorescent proteins. *Scale bars* represent 200 nm

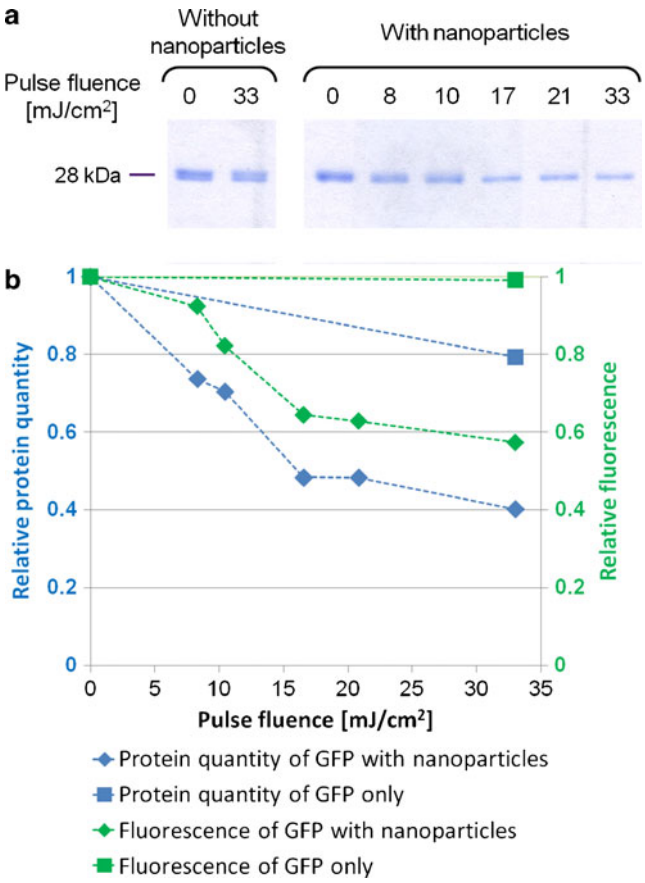

Fig. 4 **a** GFP bands in gel electrophoresis of solutions illuminated by a single pulse. **b** Plots of the relative fluorescence signals (*green*) and the GFP band intensities (*blue*) of solutions containing gold nanoparticles and GFP (*diamonds*), or GFP only (*squares*) as a function of pulse fluence. *Dashed lines* are shown as guides

weakening of the total fluorescence signal from the entire sample volume (green diamonds). Without nanoparticles, an illuminated control sample exhibited negligible decrease in fluorescence (green squares) and only a small decrease in the GFP band intensity (blue squares).

Western blot analysis (primary polyclonal rabbit antibody, secondary goat anti-rabbit HRP conjugate labeling) using an antibody that specifically recognizes GFP further confirmed the reduction of the original GFP band intensity at 28 kDa following a single-pulse irradiation (Fig. 5a). More importantly, large amounts of GFP were found in the loading wells (white arrows) of nanoparticle–GFP solutions which were irradiated by 1, 2, and 5 pulses (lanes d, e, and f, respectively). These noticeable bands could be attributed to the formation of nanoparticle–GFP conjugates, but could also result from large aggregates of pure GFP which may have formed by the intense pulse and were too large to migrate through the gel matrix.

In order to prove that the newly formed bands at the loading wells of lanes d–f in Fig. 5a are gold nanoparticles coated by fluorescent proteins, we added a strong reducing agent (25 mM dithiothreitol, DTT) to the sample loading buffer, to separate between the nanoparticles and the fluorescent proteins. This resulted in a complete loss of the high molecular weight bands and a noticeable recovery of the main GFP bands at 28 kDa, ruling out the possibility of a massive protein degradation caused by the heated nanoparticles. Since high concentrations of DTT are expected to unfold GFP aggregates, and thus could not differentiate between protein adsorption on the nanoparticles and protein aggregation, we have repeated the experiment with mCherry fluorescent protein, which is similar to GFP in many ways, but has no cysteine residues which form disulfide bonds that can be reduced by DTT. The disappearance of the band from the loading well of an irradiated nanoparticle–mCherry solution (Fig. 5b, lane a, arrow) due to the addition of DTT (lane b) implies that the bands at the loading well are not protein aggregates. Additional experiments with RFP, which contains only a single cysteine residue (and hence could not form large aggregates by disulfide bonds), have shown similar disappearance of the loading well band (Supplementary Fig. S1).

When DTT was added to all nanoparticle–protein solutions after irradiation, faint bands corresponding to molecular weights in the range of 11–17 kDa have appeared (Fig. 5a, enhanced contract region), suggesting fragmentation of a small portion of the GFP molecules into smaller peptides which could still be recognized by the anti-GFP antibody. Mass spectroscopy analysis (using matrix-assisted laser desorption/ionization time of flight, Applied Biosystems) of the region

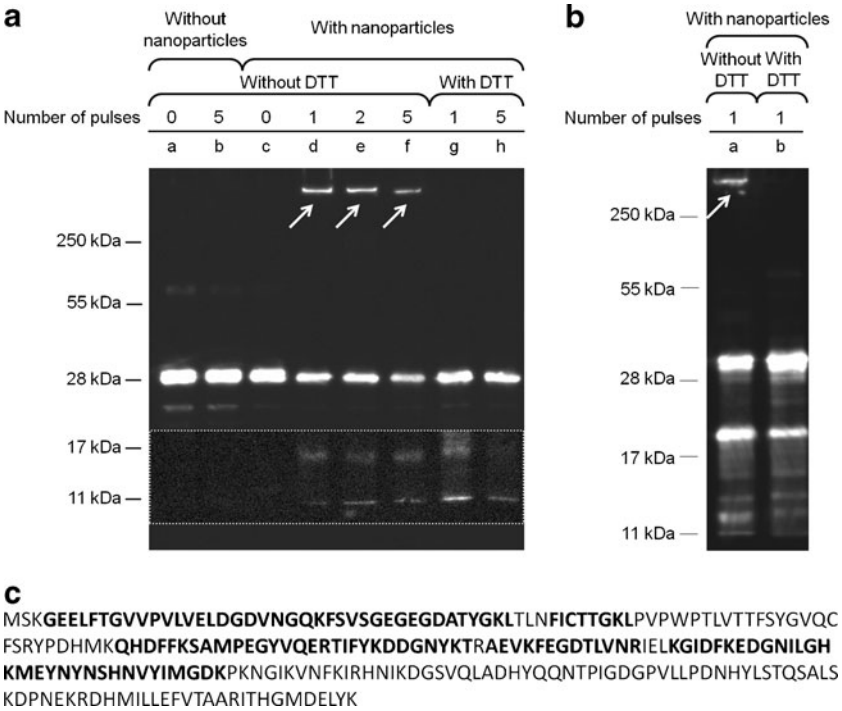

Fig. 5 **a** Western blot analysis of GFP solutions. *Lane a* GFP only; *lane b* GFP only, five-pulse irradiation; *lane c* nanoparticles + GFP; *lane d* nanoparticles + GFP, one-pulse irradiation; *lane e* nanoparticles + GFP, two-pulse irradiation; *lane f* nanoparticles + GFP, five-pulse irradiation; *lane g* nanoparticles + GFP, one pulse, added DTT; *lane h* nanoparticles + GFP, five-pulse irradiation, added DTT. The region which corresponds to molecular weights between 11 and 17 kDa (*dotted white rectangle*) was brightened (×4), and its contrast was enhanced (×10) to improve visibility of faint bands. **b** Western blot analysis of irradiated nanoparticle–mCherry solution without (*lane a*) and with (*lane b*) addition of DTT. **c** Mass spectrometry analysis of the GFP band at 17 kDa (*lane d* in **a**). Identified peptide sequences of GFP are marked by bold font

corresponding to the 17-kDa molecular weight of the irradiated nanoparticle–GFP solution (lane d in Fig. 5a) has identified various fragments of GFP (Fig. 5c), suggesting degradation of the protein through the breakage of covalent bonds. The addition of DTT to the irradiated nanoparticle–GFP solution (lane g in Fig. 5a) has resulted in a higher intensity of these bands, suggesting that some fragments of the GFP were also caught at the loading well. Excessive irradiation of the nanoparticle–GFP solution by five pulses showed considerably weaker bands at all molecular weights (lane h in Fig. 5a), suggesting massive protein degradation into small peptides comprised of only a few amino acids. Similarly, repeated single-pulse experiments with BFP, CFP, EGFP, YFP, dsRED, and mCherry showed decrease in the main protein bands in gel electrophoresis, appearance of new bands at the loading wells, and their subsequent disappearance by the addition of DTT to the sample loading buffer (supplementary Fig. S1).

Discussion

By illuminating a mixed solution of fluorescent proteins and gold nanoparticles with a single, intense optical pulse at resonance wavelength, we present a simple, yet robust, technique for the fabrication of nanoparticle–fluorescent protein conjugates. While the actual process of protein adsorption onto the nanoparticle surface is fast and requires only a single pulse, careful measurements were necessary in order to confirm the existence of such conjugates. A model which closely represents the pulse–particle–protein interaction would need to account for the experimental results described above, including the decrease in fluorescence (Fig. 2), the blue shift of the plasmonic resonance peak (Fig. 3), the decrease of the protein band intensities in gel electrophoresis (Fig. 4), and their recovery following the addition of DTT (Fig. 5a and b). During the course of this work, we have ruled out several possible explanations for the observed decrease in fluorescence; the most important one was the possible denaturation and aggregation of the protein molecules due to the mechanical and thermal energy released from the irradiated nanoparticles. Such aggregates could readily explain the rapid loss of fluorescence and the smaller protein bands in gel electrophoresis. This hypothesis, however, fails to explain the recovery of the main protein bands of the mCherry and the RFP in western blot analysis (Fig. 5b and supplementary Fig. S1), since RFP has only one cysteine residue and mCherry lacks cysteine residues, which contain the only thiol group capable of forming disulfide bonds, which in turn could be reduced by DTT. Another weakness of this model is the lack of intermediate-

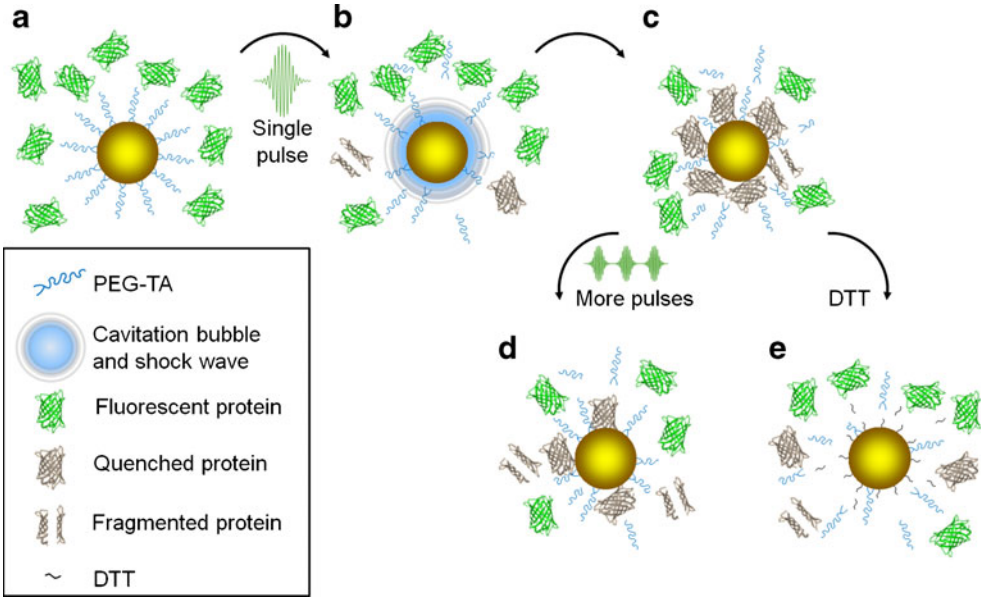

Fig. 6 Proposed model for optical pulse-driven adsorption of fluorescent proteins on gold nanoparticles. *a* Gold nanoparticles coated with PEG-TA within a solution of fluorescent proteins. *b* Irradiation by a single femtosecond pulse results in a cavitation bubble and shock wave formation, leading to partial removal of the PEG molecules. *c* The fluorescent proteins are adsorbed onto the particle, and their fluorescence is quenched. *d* Following additional pulses, the quenched proteins are gradually degraded. *e* The addition of DTT to the solution results in protein desorption from the nanoparticles

sized bands (e.g., dimers, trimers) in the gels, which would be expected from a stochastic formation of large aggregates.

Our model for representing the interaction between the light, particles, and proteins is schematically illustrated in Fig. 6. Before irradiation, the particles were chemically stable due to the PEG-TA coating layer which was linked to the particle surface by two S–Au bonds (Fig. 6, a).

After a single 50-fs optical pulse of approximately 33 mJ/cm^2 at resonance wavelength (545 nm), the irradiated 20-nm-diameter gold nanoparticles rapidly heat above their melting temperature, which may result in small shockwaves of rapidly expanding vapor bubbles [28, 58]. The released energy from the plasmonic interaction can induce gold–sulfur bond breaking [59], partially removing the PEG coating layer [60] (Fig. 6, b). With no fluorescent proteins in the irradiated solutions, massive nanoparticle aggregation was observed (see Fig. 3, right inset). In the presence of fluorescent protein molecules, however, the PEG coating of the illuminated particles was replaced by the proteins which were adsorbed onto the cooling particle surfaces (Fig. 6, c), preventing nanoparticle aggregation (see Fig. 3, left inset). The mechanism by which proteins and peptides adhere to gold surfaces [46] depends on various parameters, including the availability of side chains and functional groups with high affinity to gold, as well as the proteins' three-dimensional structure [61–63]. In similar experiments with streptavidin and myoglobin, two proteins that normally do not fluoresce and are very different from the group of fluorescent proteins in this work, we have observed no protein adsorption on the nanoparticles after irradiation, which resulted in a massive nanoparticle aggregation (Fig. 3).

The newly formed protein-coated nanoparticles (estimated molecular weight higher than 5×10^4 kDa) were too large to effectively migrate through the gel matrix and remained within the loading well (arrows in Fig. 5a). The observed blue shift and narrowing of the plasmonic peak could be attributed mainly to the increased uniformity of the nanoparticles following the intense pulse [36]. With the irradiation of additional pulses (Fig. 6, d), further degradation and defragmentation of the proteins which were already adsorbed on their surface were evident (Fig. 5a, lanes d–h). Finally, the addition of DTT, which has two SH residues and competes with the fluorescent proteins for gold nanoparticle binding, to the nanoparticle–protein solutions after irradiation has led to the desorption of the protein molecules from the nanoparticle (Fig. 6, e) and their subsequent replacement by the stabilizing DTT molecules [64].

The main advantage of the laser-triggered particle–protein conjugation presented in this work is its relative simplicity: the decoupling between the production of the gold particles, their initial coating, and the subsequent optical adsorption of selected fluorescent proteins allow control and flexibility throughout the fabrication process. Furthermore, the optical trigger could be chosen so as to optimize a certain parameter; for example, a certain amount of the original coating layer could be left on the particles if a less intense pulse is used. Different pulse durations would also affect the desired outcome; however, the pulse must be still shorter compared to the characteristic time of heat diffusion from the nanoparticles, which is of the order of 10 ps [27]. Longer pulses would be less effective for this task, inducing thermal-only effects on the particle and its surroundings. The high control over the exact location (focal volume of the beam) and timing (pulse triggering) of the adsorption process would allow accurate triggering or probing of local interactions. While the pulse irradiation affects mainly the molecules on the particle surface, it is also sufficiently

intense to cause changes to the particle's own morphology [36]. While useful for creating a more homogenous particle solution, this effect may limit the method only to spherical particles, as other particles such as nanorods could lose their shape and consequently their unique optical properties [35]. Finally, multiple optical fabrication steps for the adsorption of several layers of molecules would be difficult to execute due to the observed degradation of the proteins adjacent to the nanoparticle surface; such an additional coating layer would need to be deposited chemically.

Conclusions

In summary, we have established a new method for triggering and controlling the adsorption of various fluorescent proteins on gold nanoparticles, using intense single ultrashort pulses with wavelength that was tuned to the plasmonic resonance of the nanoparticles. By continuously monitoring the fluorescence signals, our approach offers a real-time feedback for studying and analyzing the resulting chemical interactions which lead to the adsorption of the fluorescent proteins onto the gold nanoparticles' surfaces. Optical and chemical analyses have confirmed the formation of the nanoparticle–protein conjugates and negate the formation of protein aggregates. The products of those interactions would have potential benefits in various imaging and diagnostic applications [44, 45] in which fluorescent variations are utilized for sensing their nearby chemical and physical environments and for differentiating between various types of proteins and cells.

Acknowledgments The authors thank Prof. Noam Adir, Dr. Daniella Yeheskely-Hayon, Dr. Tamar Ziv, and Haneen Yameen for enlightening discussions. They acknowledge Lior Golan, Tal Shaham, and Dan Raviv for their help with the building of the experimental system, analyses of biological samples, and data analysis, respectively. This research was funded in part by the European Research Council starting grant (239986).

References

1. Daniel MC, Astruc D (2004) Gold nanoparticles: assembly, supramolecular chemistry, quantum-size-related properties, and applications toward biology, catalysis, and nanotechnology. Chem Rev 104(1):293–346. doi:10.1021/cr030698+
2. Katz E, Willner I (2004) Integrated nanoparticle-biomolecule hybrid systems: synthesis, properties, and applications. Angew Chem Int Ed 43(45):6042–6108
3. Brust M, Fink J, Bethell D, Schiffrin DJ, Kiely C (1995) Synthesis and reactions of functionalised gold nanoparticles. J Chem Soc Chem Commun 16:1655–1656
4. Glomm WR (2005) Functionalized gold nanoparticles for applications in bionanotechnology. J Dispers Sci Technol 26(3):389–414
5. Grabar KC, Freeman RG, Hommer MB, Natan MJ (1995) Preparation and characterization of Au colloid monolayers. Anal Chem 67(4):735–743. doi:10.1021/ac00100a008
6. Eck W, Craig G, Sigdel A, Ritter G, Old LJ, Tang L, Brennan MF, Allen PJ, Mason MD (2008) PEGylated gold nanoparticles conjugated to monoclonal F19 antibodies as targeted labeling agents for human pancreatic carcinoma tissue. ACS Nano 2(11):2263–2272. doi:10.1021/nn800429d
7. Jana NR, Gearheart L, Murphy CJ (2001) Seeding growth for size control of 5–40 nm diameter gold nanoparticles. Langmuir 17 (22):6782–6786. doi:10.1021/la0104323
8. Huang X, El-Sayed MA (2010) Gold nanoparticles: optical properties and implementations in cancer diagnosis and photothermal therapy. J Adv Res 1(1):13–28
9. El-Sayed IH, Huang X, El-Sayed MA (2005) Surface plasmon resonance scattering and absorption of anti-EGFR antibody conjugated gold nanoparticles in cancer diagnostics: applications in oral cancer. Nano Lett 5(5):829–834. doi:10.1021/nl050074e
10. Sokolov K, Follen M, Aaron J, Pavlova I, Malpica A, Lotan R, Richards-Kortum R (2003) Real-time vital optical imaging of precancer using anti-epidermal growth factor receptor antibodies conjugated to gold nanoparticles. Cancer Res 63(9):1999–2004
11. Loo C, Lowery A, Halas N, West J, Drezek R (2005) Immunotargeted nanoshells for integrated cancer imaging and therapy. Nano Lett 5(4):709–711. doi:10.1021/nl050127s
12. Weiss A, Preston TC, Popov J, Li Q, Wu S, Chou KC, Burt HM, Bally MB, Signorell R (2009) Selective recognition of rituximab-functionalized gold nanoparticles by lymphoma cells studied with 3D imaging. J Phys Chem C 113(47):20252–20258. doi:10.1021/jp907423z
13. Pissuwan D, Niidome T, Cortie MB (2009) The forthcoming applications of gold nanoparticles in drug and gene delivery systems. J Control Release 149(1):65–71
14. Han G, Ghosh P, Rotello VM (2007) Functionalized gold nanoparticles for drug delivery. Nanomedicine 2(1):113–123
15. Mie G (1908) Beiträge zur Optik trüber Medien, speziell kolloidaler Metallösungen. Ann Phys 330(3):377–445
16. Kelly KL, Coronado E, Zhao LL, Schatz GC (2002) The optical properties of metal nanoparticles: the influence of size, shape, and dielectric environment. J Phys Chem B 107(3):668–677. doi:10.1021/jp026731y
17. Yelin D, Oron D, Thiberge S, Moses E, Silberberg Y (2003) Multiphoton plasmon-resonance microscopy. Opt Express 11 (12):1385–1391
18. Csaki A, Garwe F, Steinbruck A, Maubach G, Festag G, Weise A, Riemann I, Konig K, Fritzsche W (2007) A parallel approach for subwavelength molecular surgery using gene-specific positioned metal nanoparticles as laser light antennas. Nano Lett 7(2):247–253. doi:10.1021/nl061966x
19. Takeda Y, Kondow T, Mafune F (2006) Degradation of protein in nanoplasma generated around gold nanoparticles in solution by laser irradiation. J Phys Chem B 110(5):2393–2397. doi:10.1021/jp058204v
20. Takeda Y, Mafune F, Kondow T (2009) Selective degradation of proteins by laser irradiation onto gold nanoparticles in solution. J Phys Chem C 113(13):5027–5030. doi:10.1021/jp809438d
21. O'Neal DP, Hirsch LR, Halas NJ, Payne JD, West JL (2004) Photothermal tumor ablation in mice using near infrared-absorbing nanoparticles. Cancer Lett 209(2):171–176. doi:10.1016/j.canlet.2004.02.004
22. Jain PK, El-Sayed IH, El-Sayed MA (2007) Au nanoparticles target cancer. Nano Today 2(1):18–29
23. Eversole D, Luk'yanchuk B, Ben-Yakar A (2007) Plasmonic laser nanoablation of silicon by the scattering of femtosecond pulses near gold nanospheres. Applied Physics a-Materials Science & Processing 89(2):283–291

24. Nedyalkov NN, Takada H, Obara M (2006) Nanostructuring of silicon surface by femtosecond laser pulse mediated with enhanced near-field of gold nanoparticles. Appl Phys Mater Sci Process 85 (2):163–168
25. Quinten M (2001) Local fields close to the surface of nanoparticles and aggregates of nanoparticles. Applied Physics B: Lasers and Optics 73(3):245–255
26. Kneipp J, Li XT, Sherwood M, Panne U, Kneipp H, Stockman MI, Kneipp K (2008) Gold nanolenses generated by laser ablation-efficient enhancing structure for surface enhanced Raman scattering analytics and sensing. Anal Chem 80(11):4247–4251
27. Ekici O, Harrison RK, Durr NJ, Eversole DS, Lee M, Ben-Yakar A (2008) Thermal analysis of gold nanorods heated with femtosecond laser pulses. J Phys D: Appl Phys 41(18):185501
28. Volkov AN, Sevilla C, Zhigilei LV (2007) Numerical modeling of short pulse laser interaction with Au nanoparticle surrounded by water. Appl Surf Sci 253(15):6394–6399
29. Lapotko D (2009) Optical excitation and detection of vapor bubbles around plasmonic nanoparticles. Opt Express 17(4):2538–2556
30. Mafune F, Kohno J, Takeda Y, Kondow T, Sawabe H (2001) Formation of gold nanoparticles by laser ablation in aqueous solution of surfactant. J Phys Chem B 105(22):5114–5120. doi:10.1021/jp0037091
31. Kabashin AV, Meunier M, Kingston C, Luong JHT (2003) Fabrication and characterization of gold nanoparticles by femtosecond laser ablation in an aqueous solution of cyclodextrins. J Phys Chem B 107(19):4527–4531. doi:10.1021/jp034345q
32. Mafune F, Kohno JY, Takeda Y, Kondow T (2002) Full physical preparation of size-selected gold nanoparticles in solution: laser ablation and laser-induced size control. J Phys Chem B 106 (31):7575–7577. doi:10.1021/jp020577y
33. Besner S, Kabashin AV, Meunier M (2007) Two-step femtosecond laser ablation-based method for the synthesis of stable and ultrapure gold nanoparticles in water. Appl Phys Mater Sci Process 88 (2):269–272
34. Besner S, Kabashin AV, Winnik FM, Meunier M (2008) Ultrafast laser based "green" synthesis of non-toxic nanoparticles in aqueous solutions. Appl Phys Mater Sci Process 93(4):955–959
35. Link S, Burda C, Nikoobakht B, El-Sayed MA (2000) Laser-induced shape changes of colloidal gold nanorods using femtosecond and nanosecond laser pulses. J Phys Chem B 104(26):6152–6163
36. Warshavski O, Minai L, Bisker G, Yelin D (2011) Effect of single femtosecond pulses on gold nanoparticles. J Phys Chem C 115 (10):3910–3917. doi:10.1021/jp110348x
37. Amendola V, Meneghetti M (2007) Controlled size manipulation of free gold nanoparticles by laser irradiation and their facile bioconjugation. J Mater Chem 17:4705–4710. doi:10.1039/b709621f
38. Muto H, Miyajima K, Mafune F (2008) Mechanism of laser-induced size reduction of gold nanoparticles as studied by single and double laser pulse excitation. J Phys Chem C 112(15):5810–5815. doi:10.1021/jp711353m
39. Thomas KG, Kamat PV (2003) Chromophore-functionalized gold nanoparticles. Accounts of Chemical Research 36(12):888–898
40. Gersten J, Nitzan A (1981) Spectroscopic properties of molecules interacting with small dielectric particles. J Chem Phys 75 (3):1139–1152
41. Ruppin R (1982) Decay of an excited molecule near a small metal sphere. J Chem Phys 76(4):1681–1684
42. Dulkeith E, Morteani AC, Niedereichholz T, Klar TA, Feldmann J, Levi SA, van Veggel F, Reinhoudt DN, Moller M, Gittins DI (2002) Fluorescence quenching of dye molecules near gold nanoparticles: radiative and nonradiative effects. Phys Rev Lett 89 (20):4
43. Dulkeith E, Ringler M, Klar TA, Feldmann J, Javier AM, Parak WJ (2005) Gold nanoparticles quench fluorescence by phase induced radiative rate suppression. Nano Lett 5(4):585–589
44. De M, Rana S, Akpinar H, Miranda OR, Arvizo RR, Bunz UHF, Rotello VM (2009) Sensing of proteins in human serum using conjugates of nanoparticles and green fluorescent protein. Nat Chem 1(6):461–465. doi:10.1038/nchem.334
45. Bajaj A, Rana S, Miranda OR, Yawe JC, Jerry DJ, Bunz UHF, Rotello VM (2010) Cell surface-based differentiation of cell types and cancer states using a gold nanoparticle-GFP based sensing array. Chem Sci 1(1):134–138. doi:10.1039/c0sc00165a
46. Sanpui P, Pandey SB, Ghosh SS, Chattopadhyay A (2008) Green fluorescent protein for in situ synthesis of highly uniform Au nanoparticles and monitoring protein denaturation. J Colloid Interface Sci 326(1):129–137
47. Petersen S, Jakobi J, Barcikowski S (2009) In situ bioconjugation —novel laser based approach to pure nanoparticle-conjugates. Appl Surf Sci 255(10):5435–5438
48. Mafuné F, Kohno JY, Takeda Y, Kondow T, Sawabe H (2000) Formation and size control of silver nanoparticles by laser ablation in aqueous solution. J Phys Chem B 104(39):9111–9117
49. Sylvestre J-P, Poulin S, Kabashin AV, Sacher E, Meunier M, Luong JHT (2004) Surface chemistry of gold nanoparticles produced by laser ablation in aqueous media. J Phys Chem B 108 (43):16864–16869. doi:10.1021/jp047134+
50. Petersen S, Barcikowski S (2009) Conjugation efficiency of laser-based bioconjugation of gold nanoparticles with nucleic acids. J Phys Chem C 113(46):19830–19835. doi:10.1021/jp905962f
51. Wuelfing WP, Gross SM, Miles DT, Murray RW (1998) Nanometer gold clusters protected by surface-bound monolayers of thiolated poly(ethylene glycol) polymer electrolyte. J Am Chem Soc 120(48):12696–12697. doi:10.1021/ja983183m
52. Otsuka H, Nagasaki Y, Kataoka K (2003) PEGylated nanoparticles for biological and pharmaceutical applications. Adv Drug Deliv Rev 55(3):403–419
53. Murphy CJ, Gole AM, Stone JW, Sisco PN, Alkilany AM, Goldsmith EC, Baxter SC (2008) Gold nanoparticles in biology: beyond toxicity to cellular imaging. Accounts of Chemical Research 41(12):1721–1730. doi:10.1021/ar800035u
54. Daniel M-C, Astruc D (2003) Gold nanoparticles: assembly, supramolecular chemistry, quantum-size-related properties, and applications toward biology, catalysis, and nanotechnology. Chem Rev 104(1):293–346. doi:10.1021/cr030698+
55. Min I-H, Choi L, Ahn K-S, Kim BK, Lee BY, Kim KS, Choi HN, Lee W-Y (2010) Electrochemical determination of carbohydrate-binding proteins using carbohydrate-stabilized gold nanoparticles and silver enhancement. Biosens Bioelectron 26(4):1326–1331
56. Rosi NL, Mirkin CA (2005) Nanostructures in biodiagnostics. Chem Rev 105(4):1547–1562. doi:10.1021/cr030067f
57. Fujiwara H, Yanagida S, Kamat PV (1999) Visible laser induced fusion and fragmentation of thionicotinamide-capped gold nanoparticles. J Phys Chem B 103(14):2589–2591. doi:10.1021/jp984429c
58. Kotaidis V, Dahmen C, von Plessen G, Springer F, Plech A (2006) Excitation of nanoscale vapor bubbles at the surface of gold nanoparticles in water. J Chem Phys 124(18):184702–184707
59. Jain PK, Qian W, El-Sayed MA (2006) Ultrafast cooling of photoexcited electrons in gold nanoparticle-thiolated DNA conjugates involves the dissociation of the gold-thiol bond. J Am Chem Soc 128(7):2426–2433. doi:10.1021/ja056769z
60. Yamashita S, Niidome Y, Katayama Y, Niidome T (2009) Photochemical reaction of poly(ethylene glycol) on gold nanorods

induced by near infrared pulsed-laser irradiation. Chem Lett 38 (3):226–227
61. Peelle BR, Krauland EM, Wittrup KD, Belcher AM (2005) Design criteria for engineering inorganic material-specific peptides. Langmuir 21(15):6929–6933. doi:10.1021/la050261s
62. Brown S (1997) Metal-recognition by repeating polypeptides. Nat Biotech 15(3):269–272
63. Kim J, Rheem Y, Yoo B, Chong Y, Bozhilov KN, Kim D, Sadowsky MJ, Hur H-G, Myung NV (2010) Peptide-mediated shape- and size-tunable synthesis of gold nanostructures. Acta Biomater 6 (7):2681–2689
64. Wang L, Bai J, Huang P, Wang H, Zhang L, Zhao Y (2006) Self-assembly of gold nanoparticles for the voltammetric sensing of epinephrine. Electrochem Commun 8(6):1035–1040